Journal of Power Sources 444 (2019) 227227

Contents lists available at ScienceDirect

Journal of Power Sources

journal homepage: www.elsevier.com/locate/jpowsour

Short communication

An in situ system for simultaneous stress measurement and optical observation of silicon thin film electrodes

Jian Chen [a], Le Yang [b,*], Yu Han [a], Yin-Hua Bao [c], Kai-Lun Zhang [a], Xiang Li [d], Jing Pang [d], Hao-Sen Chen [a,**], Wei-Li Song [a], Yu-Jie Wei [e], Dai-Ning Fang [a,c]

[a] State Key Laboratory of Explosion Science and Technology, Institute of Advanced Structure Technology, Beijing Institute of Technology, Beijing, 100081, China
[b] AML, CNMM, Department of Engineering Mechanics, Tsinghua University, Beijing, 100084, China
[c] State Key Laboratory for Turbulence and Complex System, College of Engineering, Peking University, Beijing, 100871, China
[d] China Automotive Battery Research Institute Co., Ltd., Beijing, 100088, China
[e] LNM, Institute of Mechanics, Chinese Academy of Sciences, Beijing, 100190, China

HIGHLIGHTS

- Simultaneous stress measurement and optical observation system for Si electrode.
- Correction of theoretical expansion thickness of Si film by colorimetric method.
- Stress evolution by multi optical sensor setup and correction expansion thickness.

ARTICLE INFO

Keywords:
Lithium ion batteries
Silicon film
Multi-beam optical sensor (MOS)
In situ stress measurement
Colorimetric method

ABSTRACT

Here an in situ system is presented to simultaneously study the evolution of both morphology and stress in the silicon thin film electrode during lithiation and delithiation. Owing to the specific design with two observation windows in the in situ cell, both the curvature and color of the silicon thin-film electrodes upon lithiation and delithiation processes can be measured by multi-optical sensor and optical microscope. By such colorimetric method, the color evolution can be used to represent the thickness of silicon thin film electrode, and the quantitative relationship can be obtained by in situ atomic force microscope and optical microscopy experiments. Combining the real thickness with Stoney equation, the accurate stress of the Li_xSi film can be obtained during the electrochemical cycles.

1. Introduction

Lithium ion batteries (LIBs) are widely used in many fields, including the traditional consumer electronics, electric vehicles and the storage of renewable energy. Silicon based material is considered to be one of the most promising choices for the next generation of high energy density negative electrodes due to its high specific capacity [1]. However, the material suffers from huge volume change (~300%) [2]during electrochemical processes, which results in mechanical property reduction, diffusion induced stress, electrode damage and capacity fading of the batteries [3]. Thus, it is meaningful to accurately measure the real-time stress and morphology evolution of silicon electrodes during electrochemical cycles.

Lots of experimental methods have been made to in situ reveal the stress/strain field of the electrodes inner the batteries, such as the digital image correlation (DIC) [4–7], multi optical sensor (MOS) [8–15], laser beam probe detector (LBPD) [16] and fiber optical sensor (FOS) [17]. Among these methods, only the MOS method could directly give the average stress evolution of the electrodes, and the other methods could indirectly provide the stress, which is calculated from the collected local/average strain of the electrodes. The MOS method is based on the Stoney equation [18], and the curvature of the substrate is used to calculate stress in a film deposited on it. In the past, this in situ method has been developed and applied in various electrochemical systems [8,9,19–25].

Although the MOS method could directly obtain the stress inner the

* Corresponding author.
** Corresponding author.
E-mail addresses: yangle@tsinghua.edu.cn (L. Yang), chenhs@bit.edu.cn (H.-S. Chen).

https://doi.org/10.1016/j.jpowsour.2019.227227
Received 21 May 2019; Received in revised form 21 September 2019; Accepted 28 September 2019

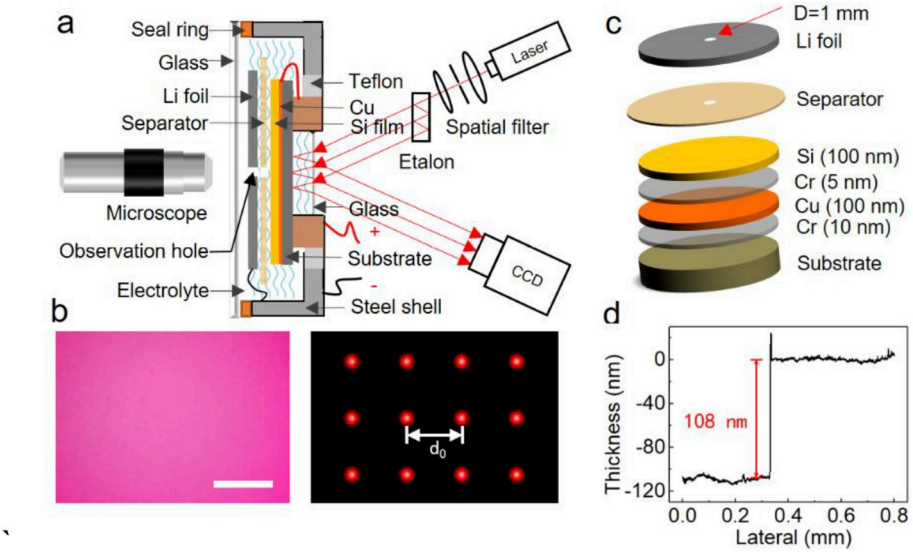

Fig. 1. (a) In situ stress measurement/optical microscopy system; (b) Optical microscope records color evolution and MOS setup monitors the relative change in the laser-spot spacing; (c) Schematic of the layered structure of the silicon film, the observation hole diameter is 1 mm; (d) The silicon film thickness is about 108 nm. The scale bar is 50 μm. (For interpretation of the references to color in this figure legend, the reader is referred to the Web version of this article.)

film, there are still some problems about the accuracy of the stress measurement, which are result from the simplified theoretical model. The thickness evolution of silicon film electrode would significantly influence the value of the stress measurement calculation. In the previous work, the thickness evolution of silicon film was determined by the theoretical volumetric deformation, which possesses a linear relationship with the Li concentration inner the electrode, and the concentration was calculated from the charge-discharge curve [14]. Compared with coin-cell, the MOS in situ battery is larger, filled by more electrolyte and more surfaces of the stainless steel shell was contacted with the electrolyte. Thus, more lithium ions would be consumed by the side reactions at the interfaces of electrolyte and the in situ battery shell. The real amount of inserted Li in the negative electrode is different from the external circuit calculation. Therefore, a more accurate method to calculate the thickness evolution of silicon film is needed. By using Focused Ion Beam(FIB), Vlassak et al. reported a method to test the thickness of silicon film under different state of charge (SOC), and determined SOC based on silicon thickness instead of the lithiation time [26]. Previously, we have developed the colorimetric method of the silicon film [27], and the relationship between color and thickness evolution of silicon film was established. During cycle, the accurate thickness can be simultaneously obtained, and combined with the Stoney equation, the more accurate stress inner the silicon film electrode can be calculated.

In this paper, an in situ experimental system for performing simultaneous morphology observation and stress measurement for silicon electrode of lithium-ion battery. The optical microscopy is used to observe the color evolution of silicon film, and the real thickness is directly extracted from the relationship of color and film thickness. Meanwhile, the curvature of the silicon electrode substrate was measured by the MOS method during the electrochemical cycles. Finally, the curvature and thickness data are substituted to the Stoney equation for the calculation of more accurate stress evolution. The advantage of our method is that the curvature and color evolution can be synchronously obtained, and the thickness evolution is obtained by the colorimetric method. In the past, the thickness is from capacity calculation, which is easily affected by the electrochemical environment. Our method can get curvature and thickness in real time, which is essential for stress calculation.

2. Experimental

2.1. Silicon thin film electrodes preparation

The 108 nm thick silicon film was prepared by sputter depositing after 10 nm of Gr, 100 nm of Cu and 5 nm of Gr on the 2-inch double-side polished silicon wafers, which was 350 μm thick with 300 nm grown silicon dioxide on both sides. The silicon was deposited in the sputter deposition system (Kurt J. Lesker LAB 18) using a pressure of 5 mTorr of Ar and a DC power of 100 W. The Cu film serves as current collector, while the Cr under-layer improves the adhesion between layers. The schematic of the layered structure of the silicon film is shown in Fig. 1(c) and the thickness of the silicon film under the stylus profiler is shown in Fig. 1(d).

2.2. Two-side in situ electrochemical cells fabrication

The in situ cell was assembled in a high-purity argon filled glove box (Mbraun Inc.) with H_2O and O_2 contents < 0.1 ppm. The electrolyte consisted of 1 M $LiPF_6$ in 1:1 (weight %) DMC: EC. The galvanostatic current cycling was carried out using Arbin battery testing system at 25 °C with a current of 50 μAcm^{-2} between 0.01 and 1.5 V (vs. Li/Li^+). The detailed structure of in situ system and the cell was shown in Fig. 1 (a). Two optical windows were designed on the battery, on the right side the laser could be reflected by the substrate, and on the left side the color could be observed though the millimeter-sized thru hole on the Li foil (counter and reference electrodes) and the separator, which is shown in Fig. 1(b). As shown in Fig. S1, the ex situ experiments were performed to prove the consistency of the thickness between the region of observation hole and the region covered by the lithium anode. Firstly, the colors were observed in this two regions, the optical photos shows no color difference (Fig. S1a). Further, an ex situ AFM scanning test was performed through the boundary of the hole, no significant thickness difference was found between the two regions (Fig. S1b). So we think the thickness in this two regions are consistent. Thus, the curvature of the substrate and the color of the silicon film can be simultaneously obtained by the MOS (K-Space Associates, Inc.) and optical microscope (Keyence Corporation), respectively.

Table 1
Parameters used for the stress calculation in this study.

Parameter	Definition	Value
d_f	Film diameter	50.8 mm
E_s	Young's modulus of Si (1 1 1) wafer	169 GPa [1]
h_f^0	Initial film thickness	100 nm
h_s	Wafer thickness	350 μm
ν_s	Poisson's ratio of Si (1 1 1)	0.26 [32]
B	Expansion factor	2.7 [14]

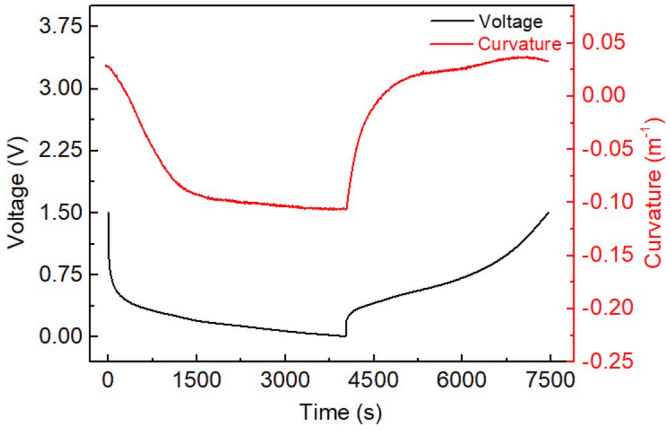

Fig. 2. Evolution of cell voltage and the curvature of substrate as a function of time during the second cycle.

2.3. Average stress calculation

The stress in the film is calculated from the curvature of the substrate using Stoney equation,

$$\sigma_f = \sigma_r + \frac{E_s h_s^2}{6h_f(1-\nu_s)}\Delta\kappa \quad (1)$$

where σ_f is the average stress in the silicon film, E_s and ν_s are Young's modulus and the Poisson's ratio of the substrate respectively, Δκ is the curvature change of the substrate, and h_s is the thickness of the substrate. σ_r is the residual stress in the silicon film that develops during sputter deposition and is obtained by substrate curvature measurements before and after sputter of the film. h_f is the thickness of the silicon film. During the electrochemical cycles, the film thickness h_f is a function of SOC. Parameters used in the analyses are given in Table 1.

The curvature change of the substrate is calculated from the geometric relation,

$$\Delta\kappa = \frac{d_0 - d}{d_0}\frac{\cos\alpha}{2L}\frac{n_a}{n_e} \quad (2)$$

where d is the distance between two adjacent laser spots measured on the CCD camera, d_0 is the initial distance between the laser spots which is shown in Fig. 1(b), α is the reflection angle of the laser beams, L is the distance between the reflective surface of silicon electrode and the CCD camera. The n_a and n_e are the refraction indices of air and the electrolyte, respectively. In the calculation of the stress, $n_e = 1.42$ for the electrolyte and $n_a = 1$ for air [11]. The laser spots are recorded per 5 s during electrochemical processes.

2.4. Relationship of color and thickness of Li_xSi film

As shown in our previous work [27], in order to obtain the real evolution of the silicon film thickness h_f during the electrochemical processes, another type of in situ experiment was proceed to calibrate the relationship of thickness and color of Li_xSi film. The thickness was measured by AFM (Demission Icon, Bruker Inc.), and the color was measured by optical microscope in the glove box during galvanostatic cycling (as shown in Fig. S2). Thus, this relationship could be used in the in situ MOS and optical experiment, and the real stress could be calculated based on the Stoney equation and real h_f.

3. Results and discussion

Due to SEI formation and other complicated side reactions during the first cycle, the silicon film optical properties are unstable. After that, the color change is highly reversible [27] and the 108 nm silicon film has good mechanical properties and does not undergo fracture damage during cycling (as shown in Fig. S3). In order to avoid the influence of the SEI formation in our experiment, the color and curvature is obtained from second cycle. The initial curvature is non-zero due to the irreversible curvature caused by the residual stress after first cycle, and this results consistent with previous work [14]. Fig. 2 shows the potential and the curvature of the film plotted versus the second cycle time. During lithiation, the substrate prevents the in-plane lithiated expansion and results in compressive stress in the film. The curvature of the substrate linearly reduces, which indicates the elastic deformation stage. The film appears to reach the elastic limit at the curvature of about $-0.075\ m^{-1}$, and the curvature value tends to the plateau, which indicates the film undergoes the plastic deformation because of the increased compressive stress. The voltage and curvature simultaneously reach the end of lithiation. During delithiation, the initial unloading process is also elastic, and the curvature elastically increase until it becomes ca. $0\ m^{-1}$. Then, the film begins to plastically deform and the curvature slowly increases. Finally, the curvature almost recovers to the initial state before lithiation and this result indicates deformation of the silicon film is almost reversible during the stable electrochemical cycle. The voltage ranges are consistent with its corresponding curvature evolution. Similar to reports [28,29], the silicon film in the in situ experiments also showed poor coulombic efficiency. The part reason of the low coulombic efficiency is the material property of the silicon material. In order to complete the in situ MOS and optical experiment, the in situ battery is generally large and filled with a large amount of electrolyte, which also leads to more side reactions and a low coulombic efficiency. The cycle with relatively low rate also exhibits poor coulombic efficiency (as shown in Fig. S5). This coulombic efficiency is about 0.73.

For the calculation of the real stress evolution in the electrode, the film thickness h_f should be obtained, it is a function with the Li concentration of the electrode. Traditionally, the thickness evolution is expressed as $h_f = h_f^0(1 + \beta z)$, where h_f^0 is the initial thickness, β is the theoretical expansion factor, and z is the Li concentration in the silicon film [11]. In second cycle, affected by residual deformation and SEI, the initial thickness $h_{f\ 2nd}^0$ is more than h_f^0. It is reasonable that the thickness evolution is expressed as $h_f = h_{f\ 2nd}^0 + h_f^0\beta z$ in second cycle. However, as mentioned before, the side reaction would be more serious in the in situ battery, which possesses more interfaces and complex structure, and it would be more different between the real and "loaded" Li concentration. Thus, the correction factor A is proposed, and the modified thickness is expressed as $h_f' = h_{f\ 2nd}^0 + Ah_f^0\beta z$, which represents the relationship between the real thickness and the loaded Li concentration of the film. Besides, the previous ex situ AFM experiments have also found the slopes of thickness-Li concentration curve is different during the lithiation and delithiation process which means the correction factor A is different during the charge and discharge process [30]. This could be caused by the asymmetrical volume change, which is related to the irreversible capacity loss.

In order to obtain the correction factor, the colorimetric method is used as shown in Fig. S2, the in situ AFM experiment and optical observation is carried out, and obtain the relationship between thickness and color. In Fig. S4, the AFM results indicate the film thickness nearly

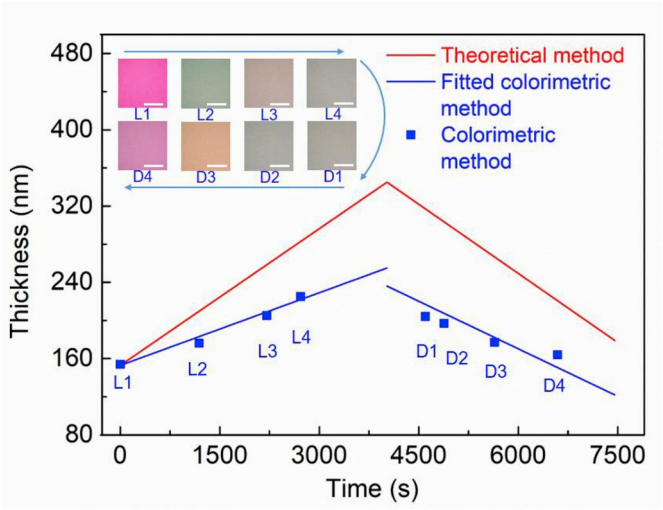

Fig. 3. Thickness evolution of Li_xSi calculated from theory (red line) and measured by colorimetric method (blue dots), and the key points color evolution. The scale bar is 30 μm. (For interpretation of the references to color in this figure legend, the reader is referred to the Web version of this article.)

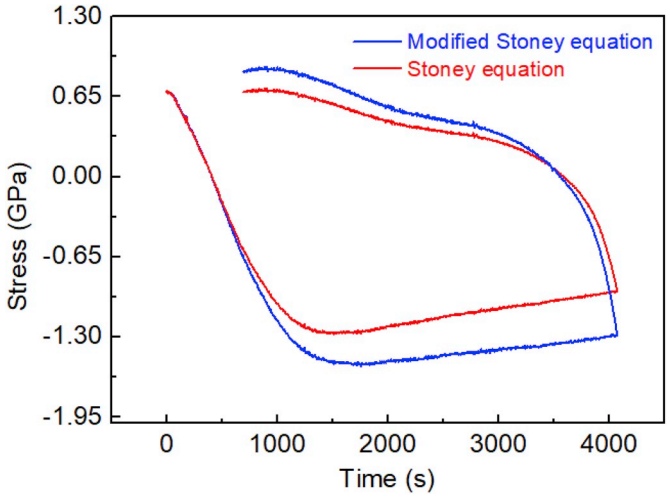

Fig. 4. Stress evolution of Li_xSi calculated from Stoney equation (red line) and modified Stoney equation (blue line). (For interpretation of the references to color in this figure legend, the reader is referred to the Web version of this article.)

linearly evoluted, which is significantly different from theoretical results. The max thickness reaches 246 nm by AFM. The difference between the two results is mainly from the large rate cycle and side reaction. As shown in Table S1, four key points were selected during charge and discharge process, respectively. Their thickness information is obtained by colorimetric experiment. It is reasonable that assume the silicon film linearly expands during lithiation and delithiation [31], and fit slopes of the thickness evolution according to the key points. Fig. 3 shows the thickness evolution and key points color change of the Li_xSi film during the second cycle, and compares the difference between theory (β is shown in Table 1) and colorimetric method for thickness evolution. Due to SEI formation, the thickness of silicon film increases to approximately 153 nm at the start of the second cycle. Upon lithiation, the height linearly expands and the maximum is 255 nm. Similarly, the height linearly shrinks during delithiation, and the height is 122 nm at the end of the second cycle. Compared to the thickness results from theory, the modified expansion results from colorimetric method are much smaller, and also indicate the loaded Li was consumed by the side reaction. At the same time, the large rate cycle also causes a large difference between the theoretical and the measured thickness value. Based on the fitting results and theory results, the lithiation and delithiation expansion factors $A_1 = 0.53$ and $A_2 = 0.81$ are obtained for the in situ MOS experiment.

Combining Figs. 2 and 3, the curvature of the electrode substrate and the modified film thickness $h_f' = h_{f\ 2nd}^0 + Ah_f^0\beta z$ is obtained. Thus, the modified stress inner the silicon film is calculated by the Stoney equation. Based on the traditional theory, the stress is also calculated as the contrast. As shown in Fig. 4, the tendency of the stress evolution is similar to the curvature in Fig. 2. However, the modified thickness evolution would significantly influence the value of the stress. The thickness of the Li_xSi film in the traditional theory was overestimated result from the neglect of the side reaction in the in situ batteries. Thus, the stress calculated from the modified thickness is higher than that calculated from the theoretical expansion factor, and the max compressive stress is 1.53 GPa which is increased 19.5% than that calculated from the traditional model. Furthermore, the max tensile stress is also increased 24.0% % to 0.88 GPa during delitiation process.

4. Conclusions

In summary, an in situ double side experimental system is presented to obtain more accurate stress evolution of silicon thin film electrode during electrochemical cycles. Based on MOS technique and colorimetric method, we introduced an in situ way to simultaneously measure the real thickness and curvature of Li_xSi thin-film during electrochemical cycles. Based on the modified thickness which includes the effect of side reaction and other influence, the modified stress inner the Li_xSi film was calculated from Stoney equation. The modified and traditional stress had similar evolution trends, both undergoing elastic stress and plastic flow. However, compared with traditional method, the modified stress exhibited larger compressive (19.5%) and tensile (24.0%) stress peak. This results suggest that the traditional method has underestimated the stress value in the electrode during electrochemical cycles. In addition, stress causes crack initiation in the thicker film electrodes. In future, we can use this system to detect stress evolution and observe crack evolution at the same time, revealing the relationship between stress and crack in electrochemical cycles.

Acknowledgments

Financial support from National Natural Science Foundation of China (Grant Nos. 11672341 and 11572002), National Key Research and Development Program of China(Grant No. 2018YFB0104400), Innovative Research Groups of the National Natural Science Foundation of China (Grant No. 11521202), National Materials Genome Project (Grant No. 2016YFB0700600), State Key Laboratory of Explosion Science and Technology (ZDKT18-03) and Beijing Natural Science Foundation (Grant Nos. 16L00001 and 2182065) is gratefully acknowledged.

Appendix A. Supplementary data

Supplementary data to this article can be found online at https://doi.org/10.1016/j.jpowsour.2019.227227.

References

[1] R. Marom, S.F. Amalraj, N. Leifer, D. Jacob, D. Aurbach, J. Mater. Chem. 21 (2011) 9938.
[2] F. Ozanam, M. Rosso, Mater. Sci. Eng., B 213 (2016) 2.
[3] S.P.V. Nadimpalli, V.A. Sethuraman, S. Dalavi, B. Lucht, M.J. Chon, V.B. Shenoy, P. R. Guduru, J. Power Sources 215 (2012) 145.
[4] W. Yang, H. Xie, B. Shi, H. Song, W. Qiu, Q. Zhang, J. Power Sources 423 (2019) 174.
[5] Y. Qi, S.J. Harris, J. Electrochem. Soc. 157 (2010) A741.
[6] E.M.C. Jones, M.N. Silberstein, S.R. White, N.R. Sottos, Exp. Mech. 54 (2014) 971.
[7] X. Cheng, M. Pecht, Energies 10 (2017) 591.

[8] J. Zhang, J. Zhang, D. Wang, X. Xie, B. Xia, Mater. Lett. 190 (2017) 79.
[9] S.P.V. Nadimpalli, V.A. Sethuraman, D.P. Abraham, A.F. Bower, P.R. Guduru, J. Electrochem. Soc. 162 (2015) A2656.
[10] V.A. Sethuraman, A. Nguyen, M.J. Chon, S.P.V. Nadimpalli, H. Wang, D. P. Abraham, A.F. Bower, V.B. Shenoy, P.R. Guduru, J. Electrochem. Soc. 160 (2013) A739.
[11] M. Pharr, Z. Suo, J.J. Vlassak, Nano Lett. 13 (2013) 5570.
[12] V.A. Sethuraman, N. Van Winkle, D.P. Abraham, A.F. Bower, P.R. Guduru, J. Power Sources 206 (2012) 334.
[13] V.A. Sethuraman, M.J. Chon, M. Shimshak, N. Van Winkle, P.R. Guduru, Electrochem. Commun. 12 (2010) 1614.
[14] V.A. Sethuraman, M.J. Chon, M. Shimshak, V. Srinivasan, P.R. Guduru, J. Power Sources 195 (2010) 5062.
[15] V.A. Sethuraman, V. Srinivasan, A.F. Bower, P.R. Guduru, J. Electrochem. Soc. 157 (2010) A1253.
[16] J.M. Rosolen, J. Electrochem. Soc. 143 (1996) 2417.
[17] C. Bae, A. Manandhar, P. Kiesel, A. Raghavan, Energy Technol-Ger 4 (2016) 851.
[18] G.G. Stoney, Proc. R. Soc. Lond. A 82 (1909) 172.
[19] J. Zhang, J. Zhang, T. Bao, X. Xie, B. Xia, J. Power Sources 348 (2017) 16.
[20] S.P.V. Nadimpalli, R. Tripuraneni, V.A. Sethuraman, J. Electrochem. Soc. 162 (2015) A2840.
[21] Y. Zhang, Y. Luo, C. Fincher, S. McProuty, G. Swenson, S. Banerjee, M. Pharr, Energy Storage Mater 16 (2019) 491.
[22] M. Pharr, Y.S. Choi, D. Lee, K.H. Oh, J.J. Vlassak, J. Power Sources 304 (2016) 164.
[23] J. Sheth, N.K. Karan, D.P. Abraham, C.C. Nguyen, B.L. Lucht, B.W. Sheldon, P. R. Guduru, J. Electrochem. Soc. 163 (2016) A2524.
[24] A. Tokranov, B.W. Sheldon, P. Lu, X. Xiao, A. Mukhopadhyay, J. Electrochem. Soc. 161 (2014) A58.
[25] M. Pharr, Z. Suo, J.J. Vlassak, J. Power Sources 270 (2014) 569.
[26] Y.S. Choi, M. Pharr, K.H. Oh, J.J. Vlassak, J. Power Sources 294 (2015) 159.
[27] Y. Bao, Y. Han, L. Yang, N. Li, J. Luo, W. Qu, R. Chen, A.K.Y. Jen, T. Li, H. Chen, W. Song, D. Fang, Adv. Funct. Mater. (2018) 1806383.
[28] S.K. Soni, B.W. Sheldon, X. Xiao, A. Tokranov, Scr. Mater. 64 (2011) 307.
[29] S.P.V. Nadimpalli, V.A. Sethuraman, G. Bucci, V. Srinivasan, A.F. Bower, P. R. Guduru, J. Electrochem. Soc. 160 (2013) A1885.
[30] Y. He, X. Yu, G. Li, R. Wang, H. Li, Y. Wang, H. Gao, X. Huang, J. Power Sources 216 (2012) 131.
[31] L.Y. Beaulieu, T.D. Hatchard, A. Bonakdarpour, M.D. Fleischauer, J.R. Dahn, J. Electrochem. Soc. 150 (2003) A1457.
[32] W.A. Brantley, J. Appl. Phys. 44 (1973) 534.